AIMS Environmental Science

AIMS Environmental Science, 12(5): 817–834.
DOI: 10.3934/environsci.2025036
Received: 01 June 2025
Revised: 03 September 2025
Accepted: 06 September 2025
Published: 17 September 2025

https://www.aimspress.com/journal/environmental

Research article

Optimization of total dissolved solids removal from produced water using a hybrid ceramic adsorbent–reverse osmosis system

Netty Herawaty[1,2], Subriyer Nasir[1,2,*], Kiagus Ahmad Roni[3] and Muhammad Rendana[4]

[1] Doctoral Engineering Program, Faculty of Engineering, Universitas Sriwijaya, Palembang 30139, South Sumatera, Indonesia
[2] Department of Chemical Engineering, Faculty of Engineering, Universitas Sriwijaya, Indralaya 30662, South Sumatera, Indonesia
[3] Chemical Engineering Study Program, Faculty of Engineering, Palembang Muhammadiyah University, Palembang 30137, South Sumatera, Indonesia
[4] Graduate Program in Chemical Engineering, Faculty of Engineering, Universitas Sriwijaya, Palembang 30139, South Sumatera, Indonesia

* **Correspondence:** Email: subriyer@unsri.ac.id; Tel: +6281279929595: Fax: +62711580303.

Abstract: Produced water (PW) is water that is extracted alongside crude oil or gas during the drilling process, necessitating proper treatment prior to environmental discharge. In this paper, we examined the application of ceramic adsorbents, derived from residue catalytic cracking (RCC) spent catalysts and natural clay, for the reduction of total dissolved solids (TDS) in PW. The preparation of ceramic adsorbents entailed the combination of spent catalyst RCC with natural clay in various proportions. The influence of adsorbent composition, diameter, flow rate, and operating time on TDS removal was investigated. Response surface methodology (RSM) was employed to optimize the removal of TDS. The findings demonstrated that a ceramic adsorbent composed of 50% RCC spent catalyst, with a diameter of 20 mm, was most effective in removing 58.39% TDS at a flow rate of PW 8 L/min. The integration of ceramic adsorbent with reverse osmosis (RO) significantly decreases the TDS of PW by 90.73%. Ceramic adsorbents are a pretreatment method for RO to decrease TDS in PW. The findings present practical implications, offering oil and gas companies an alternative method for treating PW using RCC spent catalysts and RO membrane.

Keywords: ceramic adsorbent; natural clay; spent catalyst; total dissolved solids

1. Introduction

The PW constitutes the predominant wastewater stream from reservoirs of the oil and gas industry, comprising a complex mixture of organic and inorganic compounds [1–4]. Although reinjection into an oil reservoir is the most common disposal method, PW can migrate into surface waters and soils, posing considerable environmental risks [5]. The global oil and gas sector produces around 250 million barrels of PW per day, which estimated over 40% is discharged into the environment. Typical oil wells exhibit a water-to-oil production ratio ranging between 4–5 barrels of water per barrel of oil, corresponding to roughly a 75% water cut. However, this ratio can vary widely based on reservoir characteristics, geological formation, well age, and extraction techniques [5].

The PW contains a wide range of contaminants, including salts and inorganic ions, organic acids, benzene, toluene, ethylbenzene, and xylene (BTEX) compounds, polyaromatic hydrocarbons (PAHs), phenols, metals, and chemical additives [6,7]. Treatment methods proposed for PW include oxidation processes [7], adsorption [8], membrane distillation [9], and electrochemical technologies [10]. Total dissolved solids (TDS) in PW comprise inorganic salt such as calcium, magnesium, sodium, bicarbonate, sulphate, and chlorides well as organic matter [11,12]. These constituents pose significant risks to aquatic ecosystems and water resources. Elevated TDS and salinity levels present a major challenge in PW treatment, as they can cause pipeline corrosion, hinder water reinjection, promote scaling in industrial and domestic systems, and pose potential health hazards [13,14]. Higher TDS concentrations in PW originate directly from the formation, where salinity range from 1,000 to over 300,000 mg/L [15].

Ceramic adsorbent materials are thermally and chemically stable, retain function across wide ranges of pH, temperature, and salinity, and enable tunable porosity and surface chemistry via low-cost clay formulations. These attributes make ceramics well-suited for polishing PW where durability and mass-transfer accessibility are critical [16,17]. In addition, repurposing RCC spent catalysts into clay-based ceramics advances circular-economy goals by valorizing an abundant industrial waste. Accordingly, we employe clay/RCC-based ceramic adsorbents as a scalable, low-cost, and resilient platform for PW treatment and adopt a starch-assisted formulation to generate an accessible pore network.

Adsorption is frequently employed in water and wastewater treatment because of its straightforward design, operational adaptability, high efficiency, and effective method for eliminating dissolved organic pollutants and chemical contaminants from industrial wastewater [18]. Nonetheless, a single technology is insufficient to achieve the requisite effluent characteristics in PW treatment, thereby requiring the use of multiple treatment systems in a series configuration [19,20]. Adsorption can be utilized as a hybrid or integrated process with membranes, or as a pretreatment method to improve contaminant removal and regulate flux during membrane filtration [21–24]. Membrane technology presents multiple benefits, including the elimination of superfluous chemicals, reduced energy consumption, minimized sludge generation, and the attainment of high-quality permeate water. Ceramic membranes are advantageous for industrial wastewater treatment due to their resistance to heat and chemicals, reduced fouling, extended lifespan, and versatility in composition with various metal oxides. Their high chemical and thermal stability also make them suitable for harsh environments [25,26].

Metal oxide-based catalysts are extensively utilized in the crude oil cracking process at oil refineries. Approximately 15.98 tons of catalyst are utilized annually by one of the oil and gas industries in South Sumatra, Indonesia [27]. A toxic and hazardous waste warehouse regularly disposes of and stores spent catalysts from the RCC unit. Ceramic filters have been produced utilizing the RRC spent catalyst, which comprises silica dioxide and alumina oxide, for the fabrication of ceramic filters. Researchers have conducted successful tests on ceramic filters composed of a blend of clay and RCC

spent catalyst, structured as a porous cylinder for PW treatment [28]. During the calcination process, the formation of surface cracks on ceramic filters remains an issue that can reduce their mechanical strength. Ceramic adsorbents derived from RCC and clay are regarded as alternative ceramic membranes because of their straightforward configuration, compact size, ease of fabrication, and comparable properties to traditional ceramic membranes. Ceramic adsorbents are extensively utilized for the defluorination of groundwater, water purification, and the removal of fluoride, arsenate, phosphate, and dyes. We focused on the development of ceramic adsorbents utilizing different compositions of clay and RCC-spent catalyst for the treatment of PW with TDS before the RO membrane process. Furthermore, we conducted optimization of the variables, including RCC composition in the ceramic adsorbent, diameter, contact time, and flow rate, to attain the optimal percentage of TDS reduction. A hybrid ceramic adsorbent combined with RO is anticipated to mitigate the effects of TDS on RO fouling.

2. Materials and methods

2.1. The PW collection

The PW samples were provided by oil and gas companies in South Sumatra, Indonesia. A total of 1,200 L of PW was collected in dry season to minimize seasonal variability and ensure the sample consistency before used as samples for further study. The collected PW was stored in three high density polyethylene (HDPE) tanks to ensure proper handling and prevent contamination, degradation, or leakage during storage and transport to the laboratory for subsequent treatment and analysis. Prior to being used as samples, the PW was characterized for its initial physicochemical analysis including TDS and pH using standard method.

2.2. Preparation of ceramic adsorbent

The RCC spent catalyst was obtained from a crude oil processing facility in South Sumatra, Indonesia. To synthesize the ceramic adsorbent, the RCC was first sieved using a 100-mesh screen to remove larger particulates, followed by thermal treatment in a furnace at 700–900 ℃ for one hour to eliminate hydrocarbon contaminants. Subsequently, the purified RCC was blended with natural clay in varying proportions and mixed with demineralized water to form a homogeneous paste. The resulting mixture was molded into disc-shaped tablets with diameters of 10 mm and 20 mm and a uniform thickness of 10 mm. These green bodies were oven-dried at 100 °C for 2 h and then subjected to calcination at 900–1000 ℃ overnight to enhance their structural integrity and porosity. The physicochemical properties of the synthesized adsorbents were characterized using Scanning Electron Microscopy coupled with Energy Dispersive X-ray Spectroscopy (SEM-EDX) for surface morphology and elemental composition and Brunauer–Emmett–Teller (BET) analysis to determine surface area and pore characteristics.

2.3. Composition of ceramic adsorbent

Ten cylindrical ceramic adsorbents were formulated by varying the clay to RCC ratio and pellet diameter. Percentages for clay and RCC are reported on an ash-free inorganic basis (excluding water and organic binders). Gadung starch (Dioscorea hispida) dissolved in demineralized water was added at 5 wt% relative to the total inorganic solids as a temporary binder and sacrificial pore-forming agent;

it was fully removed during thermal treatment, thereby increasing open porosity without altering the final clay: RCC ratio. Clay and RCC (both 100-mesh) were homogenized with the starch solution at room temperature to form a plastic paste (consistent with the room-temperature fabrication used in prior work on produced-water ceramics). The paste was then shaped by extrusion through circular dyes to obtain cylinders of diameters 10 and 20 mm; extrudates were cut to 10 mm thickness. Green bodies were dried at room temperature for 24 h and subsequently sintered at 900 °C for 24 h. This room-temperature drying and 900 °C sintering schedule follows produced-water ceramic filter protocols reported in the literature, ensuring methodological continuity with earlier studies [12].

Ceramic adsorbents using different raw material compositions were applied in the experiment: Adsorbent A (70% clay, 30% RCC, diameter 10 mm); B (70% clay, 30% RCC, diameter 20 mm); C (30% clay, 70% RCC, diameter 10 mm); D (30% clay, 70% RCC, diameter 20 mm); E (60% clay, 40% RCC, diameter 10 mm); F (60% clay, 40% RCC. diameter 20 mm); G (40% clay, 60% RCC, diameter 10 mm); H (40% clay, 60% RCC, diameter 20 mm); I (50% clay, 50% RCC, diameter 10 mm); and J (50% clay, 50% RCC, diameter 20 mm).

2.4. Method

Ceramic adsorbents were uniformly distributed within a polyethylene cylindrical column measuring 10 cm in diameter and 30 cm in height until full saturation was achieved. We identified three concurrent stages in the PW treatment process. The initial stage involved filtration with a polypropylene filter, followed by an adsorption stage utilizing a ceramic adsorbent, and concluding with filtration through a RO membrane. We employed the commercial CSM-RO membrane type RE 4040 BE. The RO membrane exhibited a diameter of 101.6 mm, a length of 1016 mm, and an effective area of 7.9 m². It operated at a flow rate of 9.3 m³/d, with a maximum operating pressure of 4.14 MPa (600 psi) and a maximum chloride concentration of less than 0.05 mg/L. A scanning electron microscope with energy dispersive X-ray (SEM-EDX) Hitachi Flexsem 1000 was utilized to analyze the surface morphology of the ceramic adsorbent. The TDS was measured using the Horiba Laqua PC210-K TDS Meter, while acidity was assessed using the Horiba Laqua pH meter. The formula for TDS calculation is as follows:

$$\text{TDS removal } (\%) = \frac{(\text{TDS}_{\text{in}} - \text{TDS}_{\text{out}})}{\text{TDS}_{\text{in}}} \text{ x } 100\% \quad (1)$$

where TDS_{in} shows the initial TDS of the sample, while TDS_{out} shows the TDS of the filtrate.

3. Results and discussion

3.1. Characterization of PW

Table 1 presents the characteristics of PW. The TDS values of PW surpassed the thresholds established by the Indonesian Minister of Environment regulation No. 5/2014 concerning liquid waste from oil and gas exploration. We examined TDS removal due to its substantial impact on RO membrane fouling and its potential threat to aquatic ecosystems and water intended for human use [11].

Table 1. Produced water characteristics.

Parameter	Unit	Water Quality Standard	Value
pH	-	8–9	7.82
TDS	mg/L	4,000	14,556

3.2. *Effect of ceramic adsorbent composition on acidity*

Figure 1 shows that the filtrate pH for the ceramic-adsorbent, hybrid ceramic-adsorbent, and RO streams increased relative to the PW feed yet remained within the regulatory range (6–9). All permeates were alkaline (≥ 8.0). This behavior was consistent with acid–base equilibria at oxide–water interfaces governed by the isoelectric point (IEP). When pH is larger than IEP, oxide surfaces are deprotonated and negatively charged, whereas pH less than IEP yields positive charge [29]. Typical IEPs of ~8–9 for Al_2O_3 and ~1.8–2.7 for SiO_2 explain why silica-rich surfaces are negative near neutral pH, supporting the observed association of cations (e.g., Na^+, Mg^{2+}, and K^+) at the surface. The ceramic surface is further influenced by composition and functional groups. Hydroxylated oxides such Al_2O_3, TiO_2, and ZrO_2 are intrinsically hydrophilic, which enhances wetting and facilitates water transport [23]. Across the experimental range, flow rate and contact time did not significantly affect filtrate pH (ANOVA, $P > 0.05$).

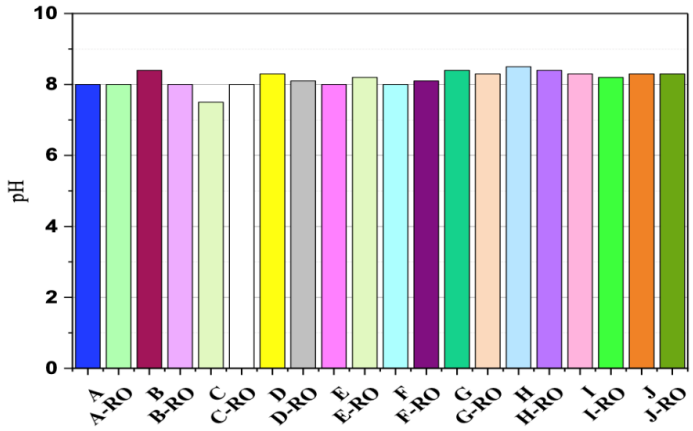

Figure 1. The pH of ceramic adsorbent effluent (A to J) and hybrid ceramic adsorbent-RO permeates (A-RO to J-RO).

SEM/EDX indicates a silica-rich surface (strong Si signal) on the ceramic adsorbent. Because silica has a low isoelectric point (≈1.8–2.7), the surface is expected to be negatively charged near neutral pH [30]. This negative charge can promote the electrostatic association of cations such as Na^+, Mg^{2+}, and K^+.

3.3. *Effects of ceramic adsorbent composition on TDS removal*

Figure 2 indicates the removal of TDS by ceramic adsorbents with dimensions of 10 mm in diameter and 10 mm in thickness. The data suggested that increasing the contact time between the adsorbent and the PW can enhance the TDS removal efficiency. Among the samples, Adsorbent A consisting of 70% clay and 30% RCC could effectively remove 71.08% of TDS. Despite this, adsorbents C, E, G, and I achieved TDS removal efficiencies of 55.65%, 55.07%, 53.21%, and 54.09%, respectively. Interestingly, a higher proportion of RCC in the ceramic adsorbent composition appered to correlate with a decline in TDS removal over time. However, the selected range of feed flow rates applied in this study showed no significant effect on TDS removal.

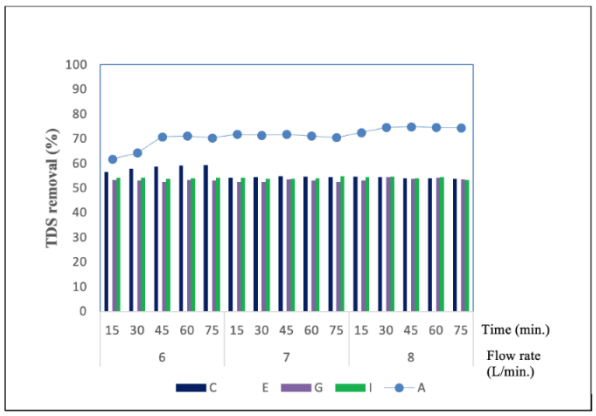

Figure 2. TDS removal (%) for different ceramic adsorbents (A C, E, G, I) at various flow times (15–75 min) and flow rates (6–8 L/min) in PW treatment using adsorbents with a diameter of 10 mm.

Figure 3 depicts TDS removal using ceramic adsorbents with a diameter of 20 mm and a thickness of 10 mm. Despite having twice the diameter compared to adsorbents A, C, E, G, and I, adsorbent B achieved a TDS removal efficiency of 55%, while adsorbents D, F, J, and H showed an average removal of 53.28% despite having twice the surface area of adsorbents A, C, E, and G. The ceramic adsorbent composition was primarily silica oxide, which had a negatively charged surface. This surface facilitated the adsorption of TDS cations through electrostatic force. At an applied flow rate, PW samples appeared to have little effect on TDS removal.

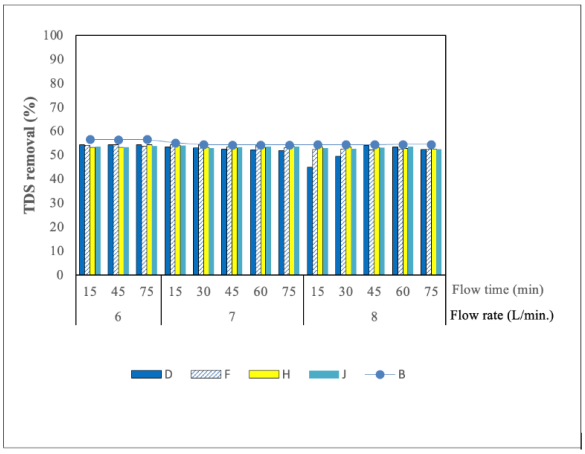

Figure 3. TDS removal (%) for ceramic adsorbents (B, D, F, H, J) at various flow times (15–75 min) and flow rates (6–8 L/min) in PW treatment using adsorbents with a diameter of 20 mm.

The TDS of PW exhibited a positive association with conductivity and influenced acidity. Various complex geological parameters of the reservoir formation, including geographical location, age, depth, and water cut, determine these values [31]. Under operating conditions of 8 L/min of flow rate and 15 minutes contact time, ceramic adsorbent D exhibited the lowest TDS removal efficiency (45.11%). Moreover, the TDS removal for ceramic adsorbent H was stable at 53.48% under the same conditions. This suggested that escalating the RCC proportion in the ceramic adsorbent may influence the adsorption

of cations on the surface of the membrane.

Figures 4 and 5 illustrate the TDS removal from PW using a hybrid system consisting of ceramic adsorbents and RO. The performance of this hybrid system, employing ceramic adsorbents with varying diameters, highlights the importance of clay content in the ceramic membrane as a key factor influencing TDS removal efficiency. As shown in Figure 4, the combination of ceramic adsorbent C and RO achieves a TDS removal efficiency ranging from 85.23% to 90.73%, indicating strong synergistic performance. Similarly, Figure 5 shows that the hybrid of ceramic adsorbent B and RO maintains a relatively consistent TDS removal efficiency between 83% and 84.1%, further supporting the effectiveness of clay-based ceramic adsorbents in hybrid systems.

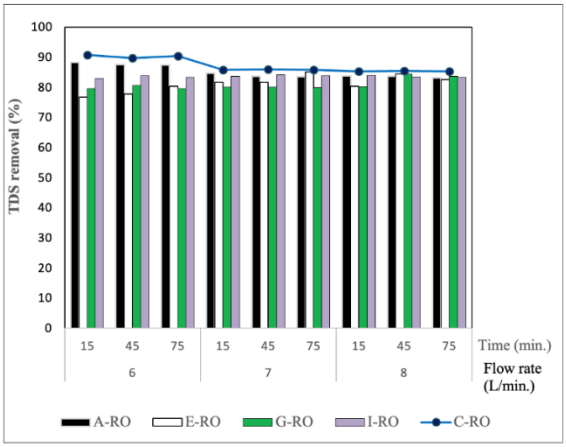

Figure 4. TDS removal (%) for hybrid ceramic adsorbent–RO systems (A–RO, C-RO, E–RO, G–RO, I–RO) at various flow times (15–75 min) and flow rates (6–8 L/min) in PW treatment using adsorbents with a diameter of 10 mm.

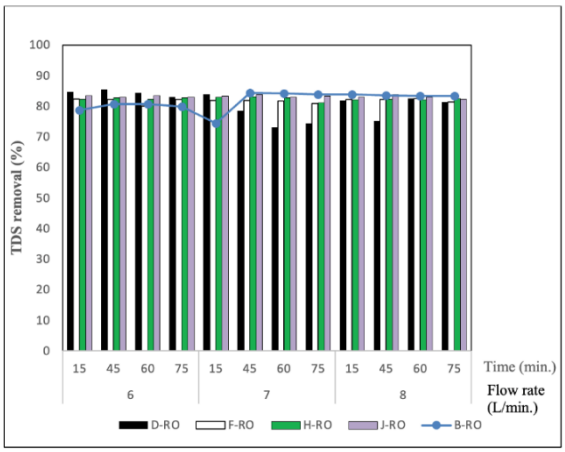

Figure 5. TDS removal (%) for hybrid ceramic adsorbent–RO systems (B–RO, D-RO, F–RO, H–RO, J–RO) at various flow times (15–75 min) and flow rates (6–8 L/min) in PW treatment using adsorbents with a diameter of 20 mm.

3.4. Effects of ceramic adsorbent diameter on TDS removal

Table 2 presents the characteristics of the RCC and ceramic adsorbents, including specific surface

area, pore size, and pore volume, determined through BET analysis based on nitrogen adsorption/desorption studies. The specific surface area was typically regarded as the primary determinant of adsorption capacity, representing a critical property in the adsorption process. Table 2 demonstrates that ceramic adsorbents with diameters of 10 mm and 20 mm exhibited specific surface areas between 10.14 and 16.55 m^2/g and 14.67 and 31.02 m^2/g, respectively. The values were lower than those of RCC, which had a surface area of 66 m^2/g and a pore size of 1.69 nm [12]. The smaller particle size of RCC compared to ceramic adsorbents contributed to its greater uniformity. The findings indicated an increase in the pore size of ceramic adsorbents from 1.69 nm to 3.79 nm. Ceramic adsorbents can be classified as mesoporous based on their pore size.

Table 2. BET characterization of ceramic adsorbents.

	Ceramic adsorbents									
	A	B	C	D	E	F	G	H	I	J
Specific surface area (m^2/g)	10.14	31.02	15.57	26.08	14.41	14.67	16.55	17.91	17.99	12.95
Pore size (nm)	3.21	1.72	1.69	1.69	3.79	3.76	2.77	2.13	1.69	3.79
Pore volume (cm^3/g)	0.03	0.06	0.04	0.07	0.05	0.05	0.05	0.05	0.05	0.05

Figure 6 illustrates the TDS concentration of PW after 75 minutes of adsorption. Among ceramic adsorbents tested, ceramic adsorbent A achieved the highest TDS removal efficiency at 74.92%. This performance could be attributed to its relatively larger pore size (with a surface area of 10.14 m^2/g) compared to other adsorbents, which was likely due to the inclusion of clay in its composition. The presence of larger pores facilitated the adsorption of cations through electrostatic interactions between the charged surface and the dissolved ions. In comparison, the hybrid system combining ceramic adsorbent C with RO attained the highest overall TDS removal of 90.73%. The use of ceramic adsorbent alone reduced TDS by approximately 54.64% from its initial level, whereas the integration of ceramic adsorption with RO consistently produced permeates meeting water quality standards, with TDS removal efficiencies ranging from 82.48% to 90.73%. In contrast, hybrid ceramic adsorbents C and RO achieved the highest TDS removal value of 90.73%.

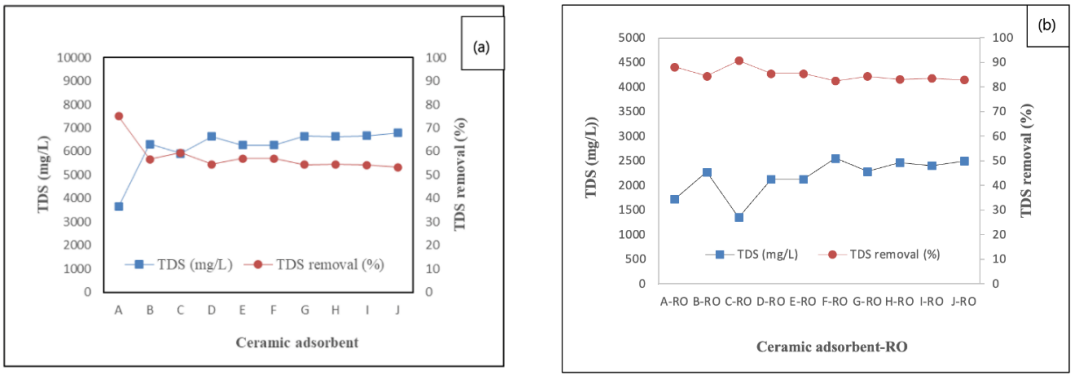

Figure 6. TDS of ceramic adsorbent filtrates (a) and hybrid ceramic adsorbent–RO permeates (b) after 75 min of treatment.

3.5. Optimization of TDS

The RSM is a statistical approach that combines experimental design techniques and is typically applied in multiple stages, including assessing the influence of factors and determining optimal conditions through the development of response surfaces and contour plots. This method enables researchers to analyze the interactions among variables and construct a predictive mathematical model that describes the overall process. Among the different RSM designs, the central composite design (CCD) is one of the most widely employed, as it efficiently supports process optimization while minimizing the number of experimental runs [30,32].

To optimize TDS removal efficiency using ceramic adsorbents, a statistical experimental design was conducted through RSM with a CCD in Minitab Software version 22. This approach enabled the evaluation of linear, interaction, and quadratic effects, which are essential for capturing complex adsorption behaviors. A total of 31 runs including factorial, axial, and center points were performed using four independent variables: RCC composition (X_1: 30–70 %), adsorbent diameter (X_2: 10 and 20 mm), adsorption time (X_3: 15–75 min), and flow rate of PW (X_4: 6–8 L/min). The relationship between these variables and TDS removal efficiency was described by a second-order polynomial regression model (Eq 2) incorporating linear, quadratic, and interaction terms:

$$Y = \beta_0 + \beta_1X_1 + \beta_2X_2 + \beta_3X_3 + \beta_4X_4 + \beta_{11}X_1^2 + \beta_{22}X_2^2 + \beta_{33}X_3^2 + \beta_{44}X_4^2 + \beta_{12}X_1X_2 + \beta_{13}X_1X_3 + \beta_{14}X_1X_4 + \beta_{23}X_2X_3 + \beta_{24}X_2X_4 + \beta_{34}X_3X_4 \quad (2)$$

Here, Y is the predicted TDS removal (%), β_0 is the intercept, β_i are the linear coefficients, β_{ii} the quadratic coefficients, and β_{ij} the interaction coefficients. Positive coefficients indicate synergistic effects, while negative ones indicate antagonistic effects.

ANOVA confirmed the model's significance ($p < 0.05$) with a high R^2 and a non-significant lack-of-fit, indicating good model adequacy. Optimization using Minitab's desirability function (target: Maximize TDS adsorption) identified the optimal conditions as RCC content 50 %, adsorbent diameter 20 mm, and flow rate 8 L/min, predicting a maximum removal of 58.39 %, which was experimentally validated with close agreement. The fitted quadratic regression equation for TDS removal is:

$$Y = 83.4 + 0.403X_1 + 0.597X_2 - 0.398X_3 - 18.6X_4 + 0.00102X_3^2 + 0.48X_4^2 - 0.05633X_1X_2 + 0.00307X_1X_3 + 0.1426X_1X_4 + 0.00335X_2X_3 + 0.3504X_2X_4 + 0.0187X_3X_4 \quad (3)$$

The positive coefficients of X_1 and X_2 indicated that increasing RCC content and adsorbent diameter enhanced TDS adsorption. Conversely, X_3 had a negative coefficient (−0.398), suggesting a slight decrease in adsorption efficiency with longer contact time, although the positive quadratic term (X_3^2) indicated the presence of a nonlinear optimum. X_4 exhibited the strongest negative linear effect (−18.6), meaning higher flow rates markedly reduced adsorption, but the positive quadratic term (X_4^2) suggested an optimal range existed. Notable interactions included X_1X_4 (0.1426) and X_2X_4 (0.3504), where simultaneous increases in these factor pairs improved adsorption. Other interactions, such as X_1X_2 and X_3X_4, had smaller coefficients and lesser influence. Overall, RCC content and adsorbent diameter were the most influential positive factors, whereas flow rate required careful control due to its strong negative linear effect combined with a quadratic optimum.

Figure 6 shows that the percentage of TDS adsorbed was significantly influenced by RCC composition, contact time, adsorbent diameter, and flow rate of PW. In general, an increase in clay consistently enhanced TDS adsorbed across all conditions. Moreover, longer contact time tended to improve adsorption, suggesting that the process occurs gradually until equilibrium is reached. A larger

adsorbent diameter also contributes to higher adsorption efficiency, likely due to an increased surface area that facilitates better interaction between the adsorbent and ions in the solution. Furthermore, higher flow rates generally enhance TDS adsorbed, but their effect is less pronounced than other factors, possibly due to limited contact time between the fluid and the adsorbent. Therefore, a combination of clay concentration, optimal contact time, larger adsorbent diameter, and an appropriate flow rate is the best condition for achieving maximum adsorption efficiency. Figure 7 shows that the surface plot confirmed the interaction between diameter and RCC on TDS adsorbed, where increasing diameter and RCC simultaneously resulted in increasing the TDS removal percentage.

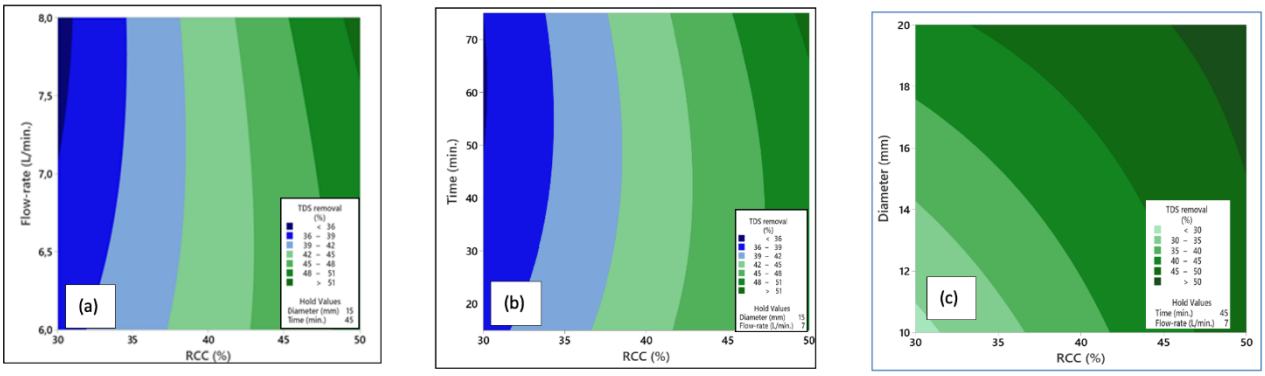

Figure 7. Contour plots RCC vs flow rate (a), time (b), and diameter (c).

3.6. Comparison with other results

Adsorption and membrane-based studies for PW treatment have reported a wide range of TDS removal efficiencies, influenced by the adsorbent type, feedwater salinity, and operating conditions, as shown in Figure 8. For instance, systems incorporating magnetite–silica nanocomposites within activated sludge processes achieved only 3.6% TDS removal [33]. Ozonation, when applied as a pretreatment step, improved membrane performance but reduced only TDS by 38.25% [34]. Constructed wetlands (CWs), developed within a circular economy framework and using materials such as aggregates, activated carbon, plastics, and shredded tires, reached 33.7% removal [35,36]. Semi-continuous bioreactor and microalgae photobioreactor systems demonstrated a moderate performance of 49.8% [37], while natural kapok fiber achieved 52% removal [13].

Intermediate performance was reported for subbituminous coal adsorbents, which achieved up to 80% removal in high-salinity waters (>150,000 mg/L) [38]. Date palm seed–based activated carbon, optimized through RSM, removed over 91% TDS alongside significant reductions in COD, BOD, and TOC [32]. Biopolymer-based composites such as chitosan–graphene also showed high efficiencies, removing 91% TDS [39]. Further improvement was observed with modified kapok fiber followed by ultrafiltration, reaching 94% TDS removal [13].

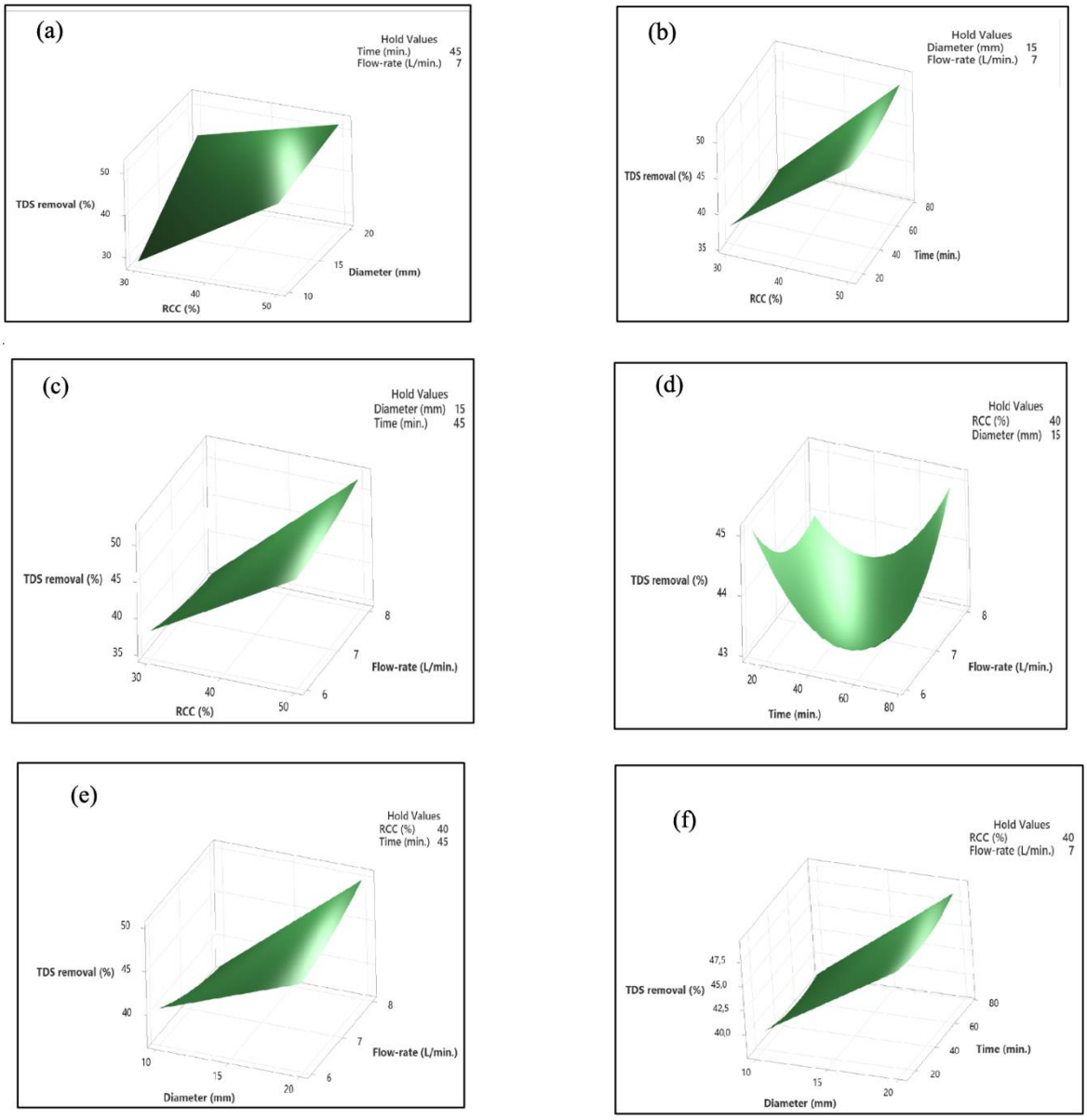

Figure 8. Surface contour plots of TDS adsorption (%) for different combinations of RCC content, adsorbent diameter, adsorption time, and flow rate.

At the upper end of performance, advanced separation technologies and hybrid processes consistently achieved near-complete TDS removal. Modified silica reduced TDS from 242,500 to 513 mg/L, corresponding to 99.8% efficiency [7]. Activated carbon pre-treatment combined with nanofiltration and RO achieved 40% and 99.67% removal, respectively [40]. Membrane distillation processes were among the most effective: Vacuum membrane distillation (VMD) reduced TDS from 138,000 to 35 mg/L (99.97%), and direct contact membrane distillation (DCMD) reduced the TDS from 135,000 to 15 mg/L (99.99%) [26,27]. Integrated treatment trains combining activated carbon, electrocoagulation, and membrane filtration produced the highest performance, removing >99% of TDS and other pollutants [41]. Overall, the comparison highlights that while adsorbent-based and nature-based systems provide moderate

reductions (30–60%), and certain advanced adsorbents reach >90%, the membrane-based and hybrid systems consistently deliver the highest TDS removal (>99%), approaching complete desalination.

Despite these advances, practical application in oilfield operations often demands materials that are not only effective in TDS reduction but also robust under extreme conditions. Ceramic-based adsorbents, including those synthesized from RCC–clay composites, offer a distinctive advantage because they combine ion-exchange and adsorption mechanisms with superior mechanical strength, chemical resistance, and thermal stability. This makes them particularly suited for treating high-TDS PW in harsh industrial environments, as they can function effectively as stand-alone units or as pretreatment to RO to reduce scaling potential and enhance overall system performance. Their versatility in composition, enabling integration of functional metal oxides, further enables tailoring of surface properties for enhanced ionic affinity, positioning ceramic-based adsorbents as a competitive solution in high-demand PW applications.

3.7. *SEM-EDX analysis of ceramic adsorbents*

The morphology of ceramic adsorbents was examined using scanning electron microscopy (SEM) and energy-dispersive X-ray spectroscopy (EDX). SEM analysis was conducted on all surfaces of the ceramic adsorbent while elemental characterizations was performed using EDX to provide detailed composition of ceramic adsorbents. Figures 9–12 illustrate the spectrum of the ceramic adsorbents before and after adsorption to illustrate their composition and SEM images of ceramic adsorbents A, B, D, and H. Ceramic adsorbents A and B were primarily composed of clay, while the RCC spent catalyst mostly consisted of ceramic adsorbents D and H. The SEM images illustrate the irregular surface and varied dimensions of the pores in the ceramic adsorbent. The EDX spectrum indicated that the ceramic adsorbents consist of silica, alumina, and iron. The ceramic adsorbent, upon usage, demonstrated the presence of sodium, magnesium, potassium, chlorine, iron, barium, and titanium ions. The acid sites present on the silica-alumina surface interacted with transition metals, including platinum and titania, among others. Clay and RCC consistuted the primary components of the ceramic adsorbent. The ceramic adsorbents confirmed the presence of silica and alumina in the RCC compounds. The characteristics of RCC resembled those of zeolite, as it consists of 38.27% silicon dioxide and 51.3% aluminum oxide, exhibiting a low Si/Al ratio of 0.75. This composition is typical of aluminosilicate materials exhibiting elevated aluminum content.

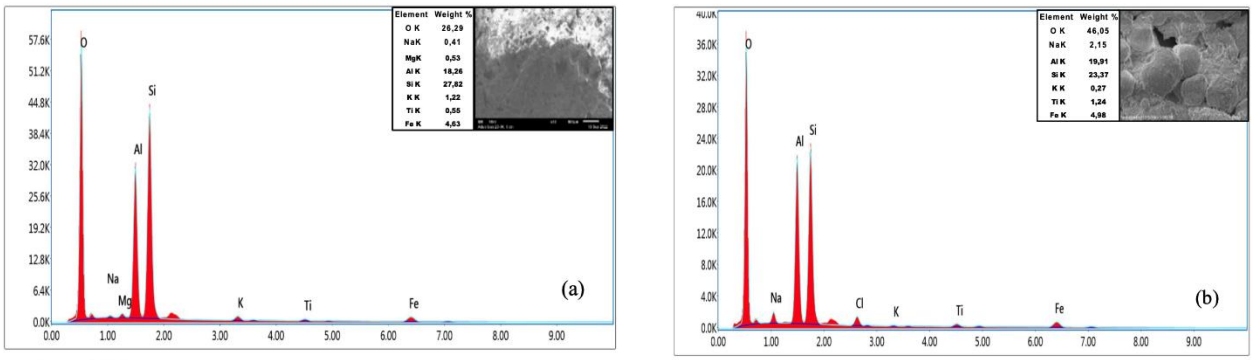

Figure 9. SEM-EDX of ceramic adsorbent A at magnification 500X before adsorption (a) and after adsorption (b).

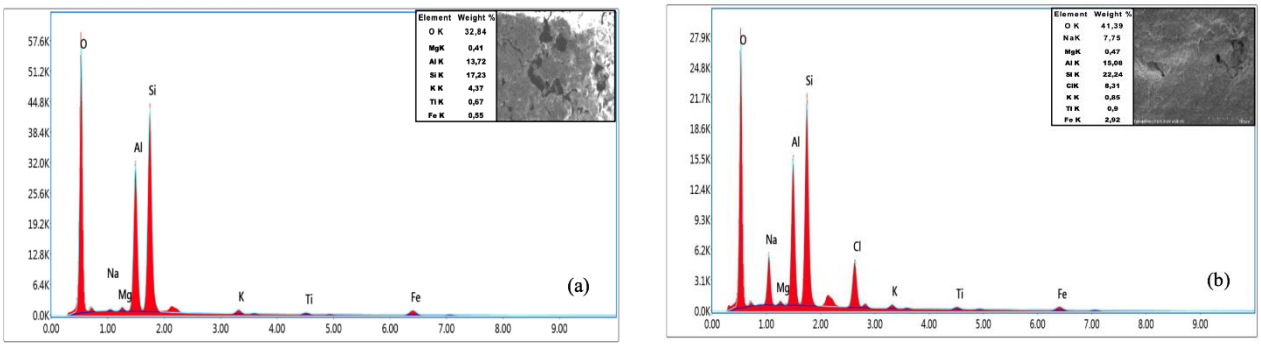

Figure 10. SEM-EDX of ceramic adsorbent B at magnification 500X before adsorption (a) and after adsorption (b).

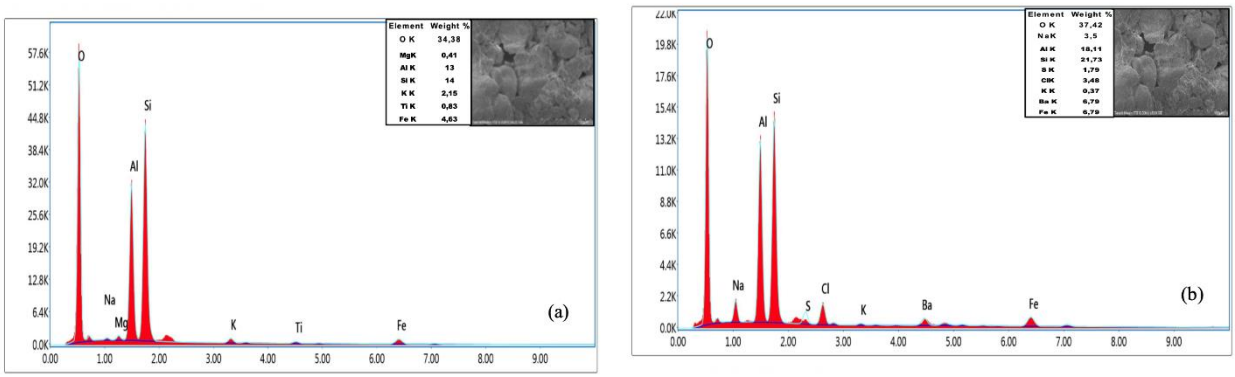

Figure 11. SEM-EDX of ceramic adsorbent D at magnification 500X before adsorption (a) and after adsorption (b).

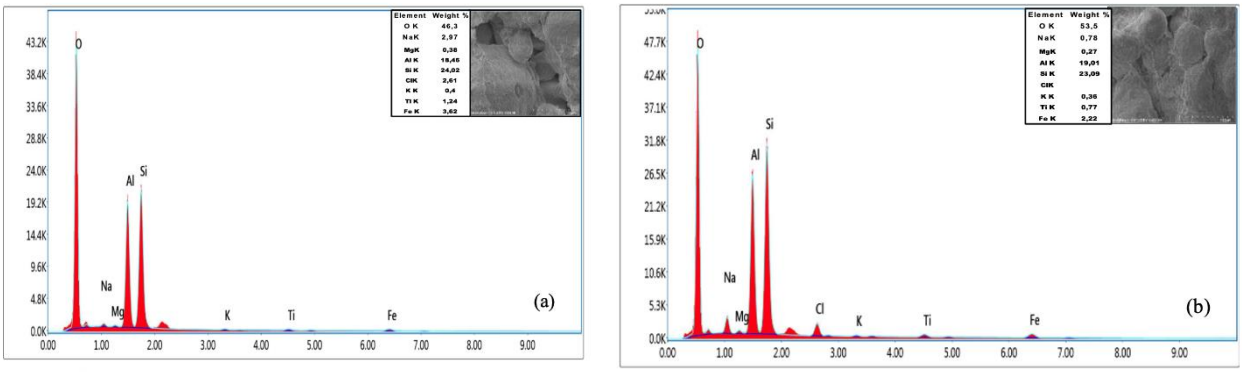

Figure 12. SEM-EDX of ceramic adsorbent H at magnification 500X before adsorption (a) and after adsorption (b).

Silicon dioxide (SiO_2) is the primary constituent of clay minerals, while aluminum oxide (Al_2O_3) is another major component. Incorporating clay into ceramic adsorbents alters the Si/Al ratio, which depends on the type of clay used. Certain clays, such as montmorillonite, have relatively high silica contents and exhibit substantially higher cation exchange capacities [36]. The presence of SiO_2 and Al_2O_3 in clay minerals contributes to adsorption capacity through ion exchange and, in the case of

expandable clays like montmorillonite, by increasing interlayer spacing, which facilitates the uptake of water and ionic species [33]. Comparison of TDS removal efficiencies for various adsorbents used in PW treatment, as shown in Figure 13.

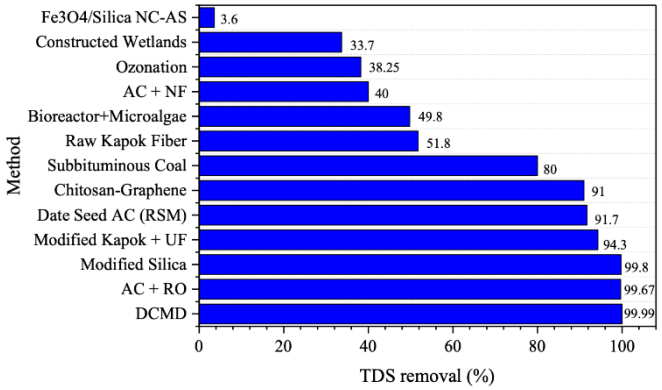

Figure 13. Comparison of TDS removal efficiencies for various adsorbents used in PW treatment.

The ANOVA for the quadratic polynomial of CCD results of TDS removal was shown in Table 3. The Si/Al ratios of the ceramic adsorbents in this study (Table 4) ranged from 1.07 to 1.58 before adsorption. In aluminosilicate-based materials, lower Si/Al ratios are generally associated with higher surface acidity, which can promote electrostatic attraction toward cations. However, in multi-component ceramics, adsorption performance is also affected by surface area, pore structure, and other oxide phases. The solution pH relative to the point of zero charge (PZC) additionally governs surface charge, which can influence cation uptake.

Table 3. ANOVA for the quadratic polynomial of CCD results of TDS removal.

Source	DF	Adj SS	Adj MS	F-Value	P-Value
Model	12	2499.3	208,275	54.2	0.000
Linear	4	1100.91	275,227	71.62	0.000
X_1	1	933.78	933,776	42.98	0.000
X_2	1	37.2	37,204	9.68	0.007
X_3	1	5.17	5,168	1.34	0.263
X_4	1	5.05	15,047	3.92	0.065
Square	2	4.29	2,143	0.56	0.583
X_1X_1	1	3.17	3,175	0.83	0.377
X_4X_4	1	1.45	1,445	0.38	0.548
2-Way Interaction	6	300.74	50,123	13.04	0.000
X_1X_2	1	195.45	195,447	50.86	0.000
X_1X_3	1	11.17	11.16	62.91	0.108
X_1X_4	1	35.77	35,768	9.31	0.008
X_2X_1	1	2.8	2,798	0.73	0.406
X_2X_4	1	49.22	49,222	12.81	0.003
X_3X_4	1	2.98	2,985	0.78	0.391

*Note: R^2 = 97.60%, Adjusted R^2 = 95.80%, and Predicted R^2 = 90.68%.

Table 4. Si/Al ratio of ceramic adsorbents.

Ceramic adsorbent	A	B	C	D	E	F	G	H
Silica/Alumina	1.46	1.21	1.07	1.08	1.58	1.47	1.20	1.25

Although this study was conducted under controlled conditions, and we focused solely on overall TDS reduction, the potential influence of coexisting impurities in PW, such as dissolved organics and oil and grease on the adsorption process, through mechanisms like fouling, competitive adsorption, or scaling, should be considered in future work to better reflect real-field conditions.

4. Conclusions

We demonstrated the potential of a hybrid ceramic adsorbent–RO system for the effective removal of TDS from PW. Optimization using RSM identified the optimum conditions as 50% RCC composition, an adsorbent diameter of 20 mm, and a flow rate of 8 L/min, achieving a maximum TDS removal efficiency of 58.39%. The statistical model showed good predictive capability, with experimental validation confirming the predicted performance. We effectively treated PW utilizing a hybrid ceramic adsorbent and RO. The spent catalyst from RCC can be utilized to produce ceramic adsorbents in diverse compositions when mixed with natural clay. Moreover, increasing the RCC content in the ceramic adsorbent composition may lead to a reduction in TDS removal from PW. The optimal TDS removal of PW is 90.73%, achieved through the use of a hybrid ceramic adsorbent C in conjunction with RO. A hybrid ceramic adsorbent combined with RO presents benefits for saline water treatment, including PW, as ceramic adsorbents are effective pretreatments for the RO process. This results from the ceramic adsorbent's capacity to decrease TDS in PW by approximately 50%. Oil and gas companies may utilize the practical implications of these findings to treat PW through the application of RCC-spent catalyst-based ceramic adsorbents and RO membranes.

Use of AI tools declaration

The authors declare they have not used Artificial Intelligence (AI) tools in the creation of this article.

Acknowledgments

The authors express their gratitude to all individuals whose contributions were invaluable in conducting this study.

Netty Herawaty, Subriyer Nasir: Conceptualization, methodology, writing original draft, writing review. Kiagus Ahmad Roni: Visualization, project administration, resources, supervision, writing original draft, writing review and editing. Muhammad Rendana: Writing review and editing.

Conflict of interest

The authors declare no competing interests.

References

1. Bezerra BGP, Parodia A, da Silva DR, et al. (2019) Cleaning produced water: A study of cation and anion removal using different adsorbents. *J Environ Chem Eng* 7: 103006. https://doi.org/10.1016/j.jece.2019.103006
2. Jiménez S, Andreozzi M, Micó MM, et al. (2019) Produced water treatment by advanced oxidation processes. *Sci Total Environ* 666: 12–21. https://doi.org/10.1016/j.scitotenv.2019.02.128
3. Ghafoori S, Omar M, Koutahzadeh N, et al. (2022) New advancements, challenges, and future needs on treatment of oilfield produced water: A state-of-the-art review. *Sep Purif Technol* 289: 120652. https://doi.org/10.1016/j.seppur.2022.120652
4. Mansi AE, El-Marsafy SM, Elhenawy Y, et al. (2023) Assessing the potential and limitations of membrane-based technologies for the treatment of oilfield produced water. *Alex Eng J* 68: 787–815. https://doi.org/10.1016/j.aej.2022.12.013
5. Rendana M, Idris WMR, Rahim SA (2022) Effect of COVID-19 movement control order policy on water quality changes in Sungai Langat, Selangor, Malaysia within distinct land use areas. *Sains Malays* 51:1587–1598. https://doi.org/10.17576/jsm-2022-5105-26
6. Jiménez S, Micó MM, Arnaldos M, et al. (2018) State of the art of treatment. *Chemosphere* 192: 186–208. https://doi.org/10.1016/j.chemosphere.2017.10.139
7. Alomar TS, Hameed BH, Usman M, et al. (2022) Recent advances on the treatment of oil fields produced water by adsorption and advanced oxidation processes. *J Water Process Eng* 49: 103034. https://doi.org/10.1016/j.jwpe.2022.103034
8. Louzada TCC, Weschenfelder SE, Passos BTD, et al. (2023) New insights in the treatment of real oilfield produced water: Feasibility of adsorption process with coconut husk activated charcoal. *J Water Process Eng* 54: 104026. https://doi.org/10.1016/j.jwpe.2023.104026
9. Chiao YH, Cao Y, Ang MBMY, et al. (2022) Application of superomniphobic electrospun membrane for treatment of real produced water through membrane distillation. *Desalination* 528: 115602. https://doi.org/10.1016/j.desal.2022.115602
10. Khorram AG, Fallah N, Nasernejad B, et al. (2023) Electrochemical-based processes for produced water and oily wastewater treatment: A review. *Chemosphere* 338: 139565. https://doi.org/10.1016/j.chemosphere.2023.139565
11. Peng J, Kumar K, Gross M, et al. (2020) Removal of total dissolved solids from wastewater using a revolving algal biofilm reactor. *Water Environ Res* 92: 766–778. https://doi.org/10.1002/wer.1273
12. Herawati N, Dahlan MH, Yusuf M, et al. (2023) Removal of total dissolved solids from oil-field-produced water using ceramic adsorbents integrated with reverse osmosis. *Mater Today Proc* 87: 3–8. https://doi.org/10.1016/j.matpr.2023.03.624
13. Rusdi E, Nasir S, Bahrin D, et al. (2023) Total dissolved solids, phenol, and barium removals from oilfield produced water using Kapok fibers and ultrafiltration membrane. *Period Polytech-Chem* 67: 452–459. https://doi.org/10.3311/PPch.21802
14. Pushpalatha N, Sreeja V, Karthik R, et al. (2022) Total dissolved solids and their removal techniques. *Int J Environ Sustai* 2: 13–30. https://doi.org/10.35745/ijesp2022v02.02.0002
15. Abdelhamid C, Latrach A, Rabiei M, et al. (2025) Produced water treatment technologies: A review. *Energies* 18: 63. https://doi.org/10.3390/en18010063
16. Xie S, Huang L, Su C, et al. (2024) Application of clay minerals as adsorbents for removing heavy metals from the environment. *Green Smart Min Eng* 1: 249–261. https://doi.org/10.1016/j.gsme.2024.07.002

17. Jarrar R, Abbas MKG, Al-Ejji M (2024) Environmental remediation and the efficacy of ceramic membranes in wastewater treatment–a review. *Emergent Mater* 7: 1295–1327. https://doi.org/10.1007/s42247-024-00687-0
18. Awad AM, Shaikh SMR, Jalab R, et al. (2019) Adsorption of organic pollutants by natural and modified clays: A comprehensive review. *Sep Purif Technol* 228: 115719. https://doi.org/10.1016/j.seppur.2019.115719
19. Houghton BDV, Liu J, Strynar MJ, et al. (2024) Performance evaluation of a high salinity produced water treatment train: Chemical analysis and Aryl hydrocarbon activation. *ACS EST Water* 4: 1293–1302. https://doi.org/10.1021/acsestwater.3c00407
20. Amakiri KT, Canon AR, Molinari M, et al. (2022) Review of oilfield produced water treatment technologies. *Chemosphere* 298: 134064. https://doi.org/10.1016/j.chemosphere.2022.134064
21. Foorginezhad S, Zerafat MM, Mohammadi Y, et al. (2022) Fabrication of tubular ceramic membranes as low-cost adsorbent using natural clay for heavy metals removal. *Clean Eng Technol* 10: 100550. https://doi.org/10.1016/j.clet.2022.100550
22. Wang Y, Ma B, Ulbricht M, et al. (2022) Progress in alumina ceramic membranes for water purification: Status and prospects. *Water Res* 226: 119173. https://doi.org/10.1016/j.watres.2022.118240
23. Chen M, Heijman SGJ, Rietveld LC (2024) Ceramic membrane filtration for oily wastewater treatment: Basics, membrane fouling and fouling control. *Desalination* 583: 117727. https://doi.org/10.1016/j.desal.2024.117727
24. Ren B, Liu J, Kang S, et al. (2023) Hierarchical porous ceramic adsorbents with nanofibrous-granular composite structure for efficient dye removal. *Ceram Int* 49: 19487–19494. https://doi.org/10.1016/j.ceramint.2023.03.083
25. Hakami MW, Alkhudhiri A, Al-Batty S, et al. (2020) Ceramic microfiltration membranes in wastewater treatment: Filtration behavior, fouling and prevention. *Membranes* 10: 393. https://doi.org/10.3390/membranes10120393
26. Dong Y, Wu H, Yang F, et al. (2022) Cost and efficiency perspectives of ceramic membranes for water treatment. *Water Res* 220: 118629. https://doi.org/10.1016/j.watres.2022.118629
27. Novira AA, Nasir S, Hadiah F (2023) Produced water treatment using the residue catalytic cracking (RCC) spent catalyst as ceramic filter material integrated with reverse osmosis (RO) system. *J Appl Sci Eng* 26: 403–411. https://doi.org/10.6180/jase.202303_26(3).0011
28. Putri RED, Nasir S, Hadiah F (2022) Application of ceramic filter and reverse osmosis membrane for produced water treatment. *Pollution* 8: 1103–1115. http://doi.org/10.22059/poll.2022.337380.1343
29. Lin B, Deng X, Chen J, et al. (2025) Integration of oxidation processes and ceramic membrane filtration for advanced water treatment: A review of foulant-membrane interactions. *Adv Membr* 5: 100138. https://doi.org/10.1016/j.advmem.2025.100138
30. Rehman K, Arslan M, Müller JA, et al. (2022) Operational parameters optimization for remediation of crude oil-polluted water in floating treatment wetlands using response surface methodology. *Sci Rep* 12: 4566. https://doi.org/10.1038/s41598-022-08517-1
31. Rajbongshi A, Gogoi SB (2024) A review on oilfield produced water and its treatment technologies. *Petol Res* 9: 640–656. https://doi.org/10.1016/j.ptlrs.2024.06.003
32. Karunya S, Prakas SJ, Prathapratim G, et al. (2021) Application of response surface methodology for optimizing processing conditions for the adsorption of pollutants from refinery effluent of Oman. *Res J Biotechnol* 16: 55–65.

33. Zabermawi NM, El Bestawy E (2024) Effective treatment of petroleum oil–contaminated wastewater using activated sludge modified with magnetite/silicon nanocomposite. *Environ Sci Pollut R* 31: 17634–17650. https://doi.org/10.1007/s11356-023-26557-6
34. Ratman I, Kusworo TD, Utomo DP (2021) Petroleum refinery wastewater treatment using a polysulfone-nano TiO_2 hybrid nembrane coupled with an ozonation process as a pre-treatment. *J Membr Sci Res* 7: 141–151. https://doi.org/10.22079/jmsr.2020.120097.1332
35. Waly MM, Mickovski SB, Thomson C (2023) Application of circular economy in oil and gas produced water treatment. *Sustainability* 15: 2132. https://doi.org/10.3390/su15032132
36. Sari DA, Said M, Bahrin D (2022) Removal of COD, TDS and Ammonia (NH_3-N) in produced water with electrochemical using Aluminum (Al) and Iron (Fe) electrode. *Int J Adv Sci Eng Inf Technol* 12: 290–297. https://doi.org/10.18517/ijaseit.12.1.14348
37. Khairuddin NFM, Khan N, Sankaran S, et al. (2024) Produced water treatment by semi-continuous sequential bioreactor and microalgae photobioreactor. *Bioresour Bioprocess* 11: 56 https://doi.org/10.1186/s40643-024-00775-3
38. Huang Z, Liu F, Tang M, et al. (2022) Removal of ions from produced water using Powder River Basin coal. *Int J Coal Sci Techn* 9: 60–72. https://doi.org/10.1007/s40789-022-00477-1
39. Ajmi S, Syed MA, Shaik F, et al. (2023) Treatment of industrial saline wastewater using eco-friendly adsorbents. *J Chem* 2023: 7366941. https://doi.org/10.1155/2023/7366941
40. Hussein MY, Al-Naemi ANA, AlJaberi FY (2023) Experimental study of produced water treatment using activated carbon with Aluminum Oxide nanoparticles, nanofiltration and reverse osmosis membranes. *J Ecol Eng* 24: 78–87. https://doi.org/10.12911/22998993/161231
41. Dehghani Y, Honarvar B, Azdarpour A, et al. (2021) Treatment of wastewater by a combined technique of adsorption, electrocoagulation followed by membrane separation. *Adv Environ Technol* 3: 171–183. http://doi.org/10.22104/AET.2021.5133.1394